RECEIVER-COORDINATED DISTRIBUTED TRANSMIT NULLFORMING WITH LOCAL AND UNIFIED TRACKING

D. Richard Brown III and Radu David

Worcester Polytechnic Institute, 100 Institute Rd, Worcester, MA 01609. Email: {drb,radud@wpi.edu}

ABSTRACT

A distributed coherent transmission scheme in which a cluster of cooperative transmitters form a beam toward an intended receiver while directing nulls at a number of other "protected" receivers is considered. The receivers coordinate the transmissions by estimating the channels and providing feedback to the transmit cluster to facilitate coherent transmission. Since the effective channels including carrier phase and frequency offsets are time-varying, two tracking schemes are compared: (i) "local tracking" where each receiver independently tracks its own channels from the transmit cluster and (ii) "unified tracking" where one receiver (or transmitter) tracks all of the channels in the system. The results show that, while beamforming performance is effectively unchanged, nullforming performance can be improved with unified tracking, especially over short prediction intervals and for larger networks.

***Index Terms*—** cooperative communication, distributed transmission, feedback systems, oscillator dynamics, tracking

1. INTRODUCTION

We consider the scenario in Fig. 1 where a distributed transmission cluster with N_t transmitters cooperate to form a virtual antenna array. The goal is to simultaneously steer a beam toward one intended receiver while also steering nulls toward $N_r - 1$ protected receivers. The receivers coordinate the transmissions by estimating the forward link channels and providing feedback to the transmit cluster to facilitate the calculation of appropriate linear precoding vectors.

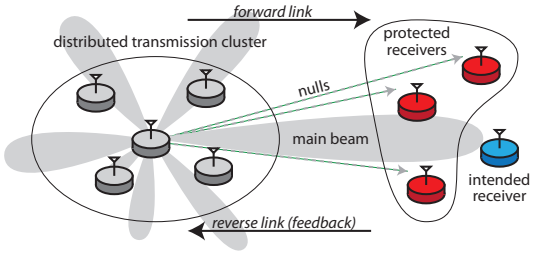

Fig. 1. Distributed transmission scenario.

The idea of distributed transmit beamforming has been well-studied in the last decade, e.g., [1–5], but the idea of distributed transmit nullforming has only recently been considered [6–8]. In particular, in [8], the approach was for each receiver to track a time-varying state of "effective" channel phase and frequency offsets which included the effect of stochastic clock drifts. Explicit state feedback from the N_r receivers was then used by the transmit cluster to predict the $N_t \times N_r$ channel matrix and compute a zero-forcing precoding vector for distributed transmission. A simplifying assumption in [8] was that each receiver *individually tracked* its N_t effective channel phase and frequency offsets. This approach is suboptimal since it does not exploit the statistical coupling of the pairwise phase and frequency offsets across all of the receive nodes.

In this paper, we study the performance of a distributed nullforming system with optimal, i.e., "unified", phase and frequency tracking at the receivers to determine the potential gains with respect to suboptimal local tracking. In practice, unified tracking could be achieved by having the receive nodes forward their observations to a master receive node and having this master receive node apply the overall observation vector to a unified Kalman filter. Alternatively, the receive nodes could provide their observations to the transmit cluster via the feedback link and one or more transmit nodes could implement a unified Kalman filter. In either case, rather than using N_r separate small Kalman filters to track the effective channel phase and frequency offsets as in [8], a system with unified tracking uses one large Kalman filter and achieves optimal performance by exploiting the correlations in the offset states across receive nodes.

This paper develops a model for unified tracking and compares the performance of this approach with respect to local tracking. Our results show that, while beamforming performance is effectively unchanged, nullforming performance can be significantly improved with unified tracking. In particular, unified tracking tends to provide the largest nullforming gains over short prediction intervals and for larger networks, e.g., distributed implementations of massive MIMO [9, 10]. The results also show that local tracking tends to provide near-optimal performance in systems with high feedback latency. We provide numerical results that confirm the analysis and compare the performance of local and unified tracking with varying prediction intervals and network sizes.

2. SYSTEM MODEL

Each node in the system shown in Fig. 1 is assumed to possess a single antenna. The nominal transmit frequency in the forward link from the distributed transmit cluster to the receivers is at ω_c. All forward link channels are modeled as narrowband, linear, and time invariant (LTI). Enumerating the transmitters as $n = 1, \ldots, N_t$ the receivers as $m = 1, \ldots, N_r$ and adopting the convention that the intended receiver is node 1, we denote the channel from transmit node n to receive node m at carrier frequency ω_c as $g^{(n,m)} \in \mathbb{C}$ for $n = 1, \ldots, N_t$ and $m = 1, \ldots, N_r$.

As in [8], all of the receivers in the system measure and track the channels from the transmit cluster and to provide feedback to the transmit cluster to facilitate distributed transmission. Fig. 2 shows the *effective* narrowband channel model from transmit node n to receive node m which includes the effects of propagation and carrier offset. Transmissions $n \to m$ are conveyed on a carrier nom-

This work was supported by the National Science Foundation awards CCF-1302104 and CCF-1319458.

inally at ω_c generated at transmit node n, incur a phase shift of $\psi^{(n,m)} = \angle g^{(n,m)}$ over the wireless channel, and are then downmixed by receive node m using its local carrier nominally at ω_c. At time t, the effective narrowband channel from transmit node n to receive node m is modeled as

$$h^{(n,m)}(\tau) = g^{(n,m)} e^{j\left(\phi_t^{(n)}(\tau) - \phi_r^{(m)}(\tau)\right)} = |g^{(n,m)}| e^{j\phi^{(n,m)}(\tau)} \quad (1)$$

where $\phi_t^{(n)}(\tau)$ and $\phi_r^{(m)}(\tau)$ are the local carrier phase offsets at transmit node n and receive node m, respectively, at time τ with respect to an ideal carrier reference, and $\phi^{(n,m)}(\tau) = \phi_t^{(n)}(\tau) - \phi_t^{(m)}(\tau) + \psi^{(n,m)}$ is the pairwise phase offset after propagation between transmit node n and receive node m at time τ.

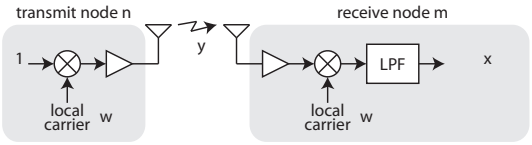

Fig. 2. Effective narrowband channel model including the effects of propagation, transmit and receive gains, and carrier offset.

2.1. Oscillator Dynamics

Each transmit and receive node in the system is assumed to have an independent local oscillator. These local oscillators have inherent frequency offsets and behave stochastically, causing phase offset variations in each effective channel from transmit node n to receive node m even when the propagation channels $g^{(n,m)}$ are otherwise time invariant. This section describes a discrete-time dynamic model to characterize the dynamics of the phase variations in $h^{(n,m)}(\tau)$.

Based on the two-state models in [11,12], we define the discrete-time state of the n^{th} transmit node's carrier as $\boldsymbol{x}_t^{(n)}[k] = [\phi_t^{(n)}[k], \dot{\phi}_t^{(n)}[k]]^\top$ where $\phi_t^{(n)}[k]$ corresponds to the carrier phase offset in radians at transmit node n with respect to an ideal carrier phase reference. The state update of the n^{th} transmit node's carrier is then

$$\boldsymbol{x}_t^{(n)}[k+1] = \boldsymbol{f}(T)\boldsymbol{x}_t^{(n)}[k] + \boldsymbol{u}_t^{(n)}[k] \text{ with } \boldsymbol{f}(T) = \begin{bmatrix} 1 & T \\ 0 & 1 \end{bmatrix} \quad (2)$$

where T is an arbitrary sampling period selected to be small enough to avoid phase aliasing at the largest expected frequency offsets. The process noise vector $\boldsymbol{u}_t^{(n)}[k] \overset{\text{i.i.d.}}{\sim} \mathcal{N}\left(\boldsymbol{0}, \boldsymbol{Q}_t^{(n)}(T)\right)$ causes the carrier derived from the local oscillator at transmit node n to deviate from an ideal linear phase trajectory. The covariance of the discrete-time process noise is derived from a continuous-time model in [11] and is

$$\boldsymbol{Q}_t^{(n)}(T) = \omega_c^2 T \begin{bmatrix} p_t^{(n)} + q_t^{(n)} \frac{T^2}{3} & q_t^{(n)} \frac{T}{2} \\ q_t^{(n)} \frac{T}{2} & q_t^{(n)} \end{bmatrix} \quad (3)$$

where ω_c is the nominal common carrier frequency in radians per second and $p_t^{(n)}$ (units of seconds) and $q_t^{(n)}$ (units of Hertz) are the process noise parameters corresponding to white frequency noise and random walk frequency noise, respectively.

The receive nodes in the system also have independent local oscillators used to generate carriers for downmixing that are governed by the same dynamics as (2) with state $\boldsymbol{x}_r^{(m)}[k]$, process noise $\boldsymbol{u}_r^{(m)}[k] \overset{\text{i.i.d.}}{\sim} \mathcal{N}(0, \boldsymbol{Q}_r^{(m)}(T))$, and process noise parameters $p_r^{(m)}$ and $q_r^{(m)}$ as in (3) for $m = 1, \ldots, N_r$.

Since receive nodes can only measure the relative phase and frequency of the transmit nodes after propagation, we define the *pairwise offset* after propagation as

$$\boldsymbol{\delta}^{(n,m)}[k] = \begin{bmatrix} \phi^{(n,m)}[k] \\ \dot{\phi}^{(n,m)}[k] \end{bmatrix} = \boldsymbol{x}_t^{(n)}[k] + \begin{bmatrix} \psi^{(n,m)} \\ 0 \end{bmatrix} - \boldsymbol{x}_r^{(m)}[k].$$

Note that $\boldsymbol{\delta}^{(n,m)}[k]$ is governed by the state update

$$\boldsymbol{\delta}^{(n,m)}[k+1] = \boldsymbol{f}(T)\boldsymbol{\delta}^{(n,m)}[k] + \boldsymbol{u}_t^{(n)}[k] - \boldsymbol{u}_r^{(m)}[k]. \quad (4)$$

We assume that observations are so short as to only provide useful phase estimates. An observation of the $n \to m$ channel is then

$$y^{(n,m)}[k] = \boldsymbol{h}\delta^{(n,m)}[k] + v^{(n,m)}[k]$$

where $\boldsymbol{h} = [1, 0]$ and $v^{(n,m)}[k] \overset{\text{i.i.d.}}{\sim} \mathcal{N}(0, R)$ is the measurement noise which is assumed to be spatially and temporally i.i.d.

2.2. Local Tracking Model

In the case of local tracking, each receiver uses only its local observations to track the pairwise offset states with respect to the receiver's local oscillator. At receiver m, the $2N_t$-dimensional vector state of pairwise offsets is defined as $\boldsymbol{\delta}^{(m)}[k] = [(\boldsymbol{\delta}^{(1,m)}[k])^\top, \ldots, (\boldsymbol{\delta}^{(N_t,m)}[k])^\top]^\top$ and has the state update

$$\begin{aligned} \boldsymbol{\delta}^{(m)}[k+1] &= \begin{bmatrix} \boldsymbol{f}(T) & & \\ & \ddots & \\ & & \boldsymbol{f}(T) \end{bmatrix} \boldsymbol{\delta}^{(m)}[k] + \begin{bmatrix} \boldsymbol{u}_t^{(1)}[k] - \boldsymbol{u}_r^{(m)}[k] \\ \vdots \\ \boldsymbol{u}_t^{(N_t)}[k] - \boldsymbol{u}_r^{(m)}[k] \end{bmatrix} \\ &= \boldsymbol{F}_{\text{loc}}(T)\boldsymbol{\delta}^{(m)}[k] + \boldsymbol{G}_{\text{loc}}\boldsymbol{u}^{(m)}[k]. \end{aligned} \quad (5)$$

where

$$\boldsymbol{G}_{\text{loc}} = \begin{bmatrix} \boldsymbol{I}_2 & & & -\boldsymbol{I}_2 \\ & \ddots & & \vdots \\ & & \boldsymbol{I}_2 & -\boldsymbol{I}_2 \end{bmatrix} \text{ and } \boldsymbol{u}^{(m)}[k] = \begin{bmatrix} \boldsymbol{u}_t^{(1)}[k] \\ \vdots \\ \boldsymbol{u}_t^{(N_t)}[k] \\ \boldsymbol{u}_r^{(m)}[k] \end{bmatrix} \quad (6)$$

and where $\boldsymbol{I}_2$ is the 2×2 identity matrix. We assume

$$\begin{aligned} \text{cov}\{\boldsymbol{u}^{(m)}[k]\} &= \text{blockdiag}\left\{\boldsymbol{Q}_t^{(1)}(T), \ldots, \boldsymbol{Q}_t^{(N_t)}(T), \boldsymbol{Q}_r^{(m)}(T)\right\} \\ &= \boldsymbol{Q}^{(m)}(T) \end{aligned}$$

hence $\boldsymbol{G}_{\text{loc}}\boldsymbol{u}^{(m)}[k] \sim \mathcal{N}\left(\boldsymbol{0}, \boldsymbol{G}_{\text{loc}}\boldsymbol{Q}^{(m)}(T)\boldsymbol{G}_{\text{loc}}^\top\right)$. The vector observation for the local Kalman filter is then $\boldsymbol{y}^{(m)}[k] = [y^{(1,m)}[k], \ldots, y^{(N_t,m)}[k]]^\top$ and related to the local state as

$$\boldsymbol{y}^{(m)}[k] = \boldsymbol{h}_{\text{loc}}\boldsymbol{\delta}^{(m)}[k] + \boldsymbol{v}^{(m)}[k]$$

where $\boldsymbol{h}_{\text{loc}} = \text{blockdiag}(\boldsymbol{h}, \ldots, \boldsymbol{h}) \in \mathbb{R}^{N_t \times 2N_t}$ and $\boldsymbol{v}^{(m)}[k] = [v^{(1,m)}[k], \ldots, v^{(N_t,m)}[k]]^\top \in \mathbb{R}^{N_t}$ is the measurement noise.

2.3. Unified Tracking Model

In the case of unified tracking, there is a master receiver or transmitter that aggregates all of the observations and tracks all of the pairwise offset states in the system. The $2N_tN_r$-dimensional vector state of pairwise offsets is defined as $\boldsymbol{\delta}[k] = [(\boldsymbol{\delta}^{(1)}[k])^\top, \ldots, (\boldsymbol{\delta}^{(N_r)}[k])^\top]^\top$ and has the state update

$$\begin{aligned} \boldsymbol{\delta}[k+1] &= \begin{bmatrix} \boldsymbol{f}(T) & & \\ & \ddots & \\ & & \boldsymbol{f}(T) \end{bmatrix} \boldsymbol{\delta}[k] + \begin{bmatrix} \boldsymbol{u}_t^{(1)}[k] - \boldsymbol{u}_r^{(1)}[k] \\ \vdots \\ \boldsymbol{u}_t^{(N_t)}[k] - \boldsymbol{u}_r^{(N_r)}[k] \end{bmatrix} \\ &= \boldsymbol{F}_{\text{uni}}(T)\boldsymbol{\delta}[k] + \boldsymbol{G}_{\text{uni}}\boldsymbol{u}[k] \end{aligned} \quad (7)$$

where the process noise vector $\boldsymbol{u}[k] = [(\boldsymbol{u}_t^{(1)}[k])^\top, \ldots, (\boldsymbol{u}_t^{(N_t)}[k])^\top, (\boldsymbol{u}_r^{(1)}[k])^\top, \ldots, (\boldsymbol{u}_r^{(N_r)}[k])^\top]^\top \in \mathbb{R}^{2(N_t+N_r)}$ and

$$\boldsymbol{G}_{\text{uni}} = \begin{bmatrix} \boldsymbol{I}_{2N_t} & \boldsymbol{J}_{2N_t} & & \\ \vdots & & \ddots & \\ \boldsymbol{I}_{2N_t} & & & \boldsymbol{J}_{2N_t} \end{bmatrix} \in \mathbb{R}^{2N_tN_r \times 2(N_t+N_r)} \quad (8)$$

with $\boldsymbol{J}_{2N_t} = -[\boldsymbol{I}_2, \ldots, \boldsymbol{I}_2]^\top \in \mathbb{R}^{2N_t \times 2}$. The N_tN_r-dimensional vector observation for the unified Kalman filter is then

$$\boldsymbol{y}[k] = \boldsymbol{h}_{\text{uni}}\boldsymbol{\delta}[k] + \boldsymbol{v}[k]$$

where $\boldsymbol{h}_{\text{uni}} = \mathsf{blockdiag}(\boldsymbol{h}, \ldots, \boldsymbol{h}) \in \mathbb{R}^{N_tN_r \times 2N_tN_r}$ and $\boldsymbol{v}[k] = [v^{(1,1)}[k], \ldots, v^{(N_t,N_r)}[k]]^\top \in \mathbb{R}^{N_tN_r}$ is the measurement noise.

2.4. Discussion

Note that the state update equations (5) and (7) specify dynamic systems where the states are coupled only through the correlated process noise. In the local tracking model, the process noise is correlated only through receive node m's oscillator as shown in (6). In the unified tracking model, the process noise is correlated through *all* of the receive oscillators as shown in (8). While the number of states grows according to the product N_tN_r, the number of independent oscillators grows according to the sum $N_t + N_r$. Hence, since the unified tracker exploits all of the process noise correlations in the system, we can expect the unified tracker to provide the most significant performance gains with respect to local tracking in large networks.

3. RECEIVER-COORDINATED PROTOCOL

We assume the receiver-coordinated protocol described in [7, 8]. Forward link transmissions are divided into measurement and distributed transmission epochs, repeating periodically with period T_m. Reverse link transmissions provide feedback from the receive nodes to the transmit nodes to facilitate linear precoding vector calculation.

Given a measurement at time k and denoting the Kalman filter's MMSE phase prediction at time $\ell > k$ as $\hat{\phi}^{(n,m)}[\ell \,|\, k]$, we can write the effective channel prediction for $h^{(n,m)}(\tau)$ at time $\tau = \ell T$ as

$$\hat{h}^{(n,m)}[\ell \,|\, k] = |g^{(n,m)}|e^{j\hat{\phi}^{(n,m)}[\ell \,|\, k]} \quad (9)$$

since the channel amplitudes $|g^{(n,m)}|$ are assumed to be known. We denote the vector of channel predictions from all transmit nodes to receive node m as $\hat{\boldsymbol{h}}^{(m)}[\ell \,|\, k] \in \mathbb{C}^{N_t}$ and the protected receiver predicted channel matrix as $\hat{\boldsymbol{H}}[\ell|k] = \left[\hat{\boldsymbol{h}}^{(2)}[\ell|k], \ldots, \hat{\boldsymbol{h}}^{(N_r)}[\ell|k]\right] \in \mathbb{C}^{N_t \times N_r}$ for $\ell > k$.

The MMSE channel predictions are used to calculate the precoding vector $\boldsymbol{w}[\ell] \in \mathbb{C}^{N_t}$ for all ℓ in the distributed transmission epoch. Under our assumption that the number of protected receivers is less than N_t, we can select the transmit vector $\boldsymbol{w}[\ell] \in \mathbb{C}^{N_t}$ to be orthogonal to $\hat{\boldsymbol{h}}^{(m)}[\ell \,|\, k]$ for all $m = 2, \ldots, N_r$ and then use the remaining degrees of freedom in the transmit vector to maximize the received power at the intended receiver. Defining $\hat{\boldsymbol{D}}[\ell|k] = \boldsymbol{I} - \hat{\boldsymbol{H}}[\ell|k]\left(\hat{\boldsymbol{H}}^H[\ell|k]\hat{\boldsymbol{H}}[\ell|k]\right)^{-1}\hat{\boldsymbol{H}}^H[\ell|k]$, the zero-forcing transmit vector can then be computed as

$$\boldsymbol{w}[\ell] = \alpha[\ell]\hat{\boldsymbol{D}}[\ell|k]\hat{\boldsymbol{h}}^{(1)}[\ell|k] \quad (10)$$

where $\alpha[\ell]$ is selected to satisfy a per-node or total power constraint.

4. PERFORMANCE ANALYSIS

This section analyzes the steady-state performance of local and unified tracking. Our analysis assumes unit channel magnitudes such that $|g^{(n,m)}| = 1$, i.i.d. measurement noise with $\boldsymbol{v}[k] \sim \mathcal{N}(0, \boldsymbol{R})$ and $\boldsymbol{R} = \sigma_v^2\boldsymbol{I}$, and identical process noise statistics at each node.

To compute the steady-state prediction covariance of the Kalman filter with measurement period T_m, it can be straightforwardly verified that both the local and unified tracking systems satisfy the controllability and observability conditions so that the steady-state prediction covariance is a unique positive definite matrix specified as the solution to the discrete-time algebraic Riccati equation [13]. Denoting the prediction covariance as $\boldsymbol{P}$ (corresponding to either local or unified tracking), the steady-state estimation covariance (immediately after an observation) is then $\boldsymbol{S} = \boldsymbol{P} - \boldsymbol{P}\boldsymbol{h}^\top(\boldsymbol{h}\boldsymbol{P}\boldsymbol{h}^\top + \boldsymbol{R})^{-1}\boldsymbol{h}\boldsymbol{P}$. The prediction covariance at a prediction time t_p after the most recent measurement (during a distributed transmission epoch) is then $\boldsymbol{P}(t_p) = \boldsymbol{F}(t_p)\boldsymbol{S}\boldsymbol{F}^\top(t_p) + \boldsymbol{Q}(t_p)$. The (1,1) element of $\boldsymbol{P}(t_p)$ is the variance of the phase prediction, which we denote as $\sigma_\phi^2(t_p)$. The (1,3) element of $\boldsymbol{P}(t_p)$ is the covariance of the phase predictions between two transmitters as observed at one receiver, which we denote as $\rho^2\sigma_\phi^2(t_p)$.

To quantify the performance of distributed *beamforming* in terms of the prediction covariance, suppose that the signal received from the i^{th} transmitter at the intended receiver is given by $r_i = \alpha e^{j(\phi+\tilde{\phi}_i)}$ where $\alpha^2 = N_t^{-1}$ is the individual transmit power selected to satisfy a unit total power constraint, ϕ is the nominal beamforming phase, and $\tilde{\phi}_i$ is the phase error at transmitter i. The mean beamforming power is then

$$J = \mathrm{E}\left\{\left|\sum_{i=1}^{N_t} r_i\right|^2\right\} = \frac{1}{N_t}\sum_{i=1}^{N_t}\mathrm{E}\left\{c_i^2 + s_i^2\right\} + \frac{1}{N_t}\sum_{i=1}^{N_t}\sum_{j\neq i}\mathrm{E}\left\{c_ic_j + s_is_j\right\}$$

where $c_i = \cos(\tilde{\phi}_i)$ and $s_i = \sin(\tilde{\phi}_i)$. Since $c_i^2 + s_i^2 = 1$ and $c_ic_j + s_is_j = \cos(\tilde{\phi}_i - \tilde{\phi}_j)$, we have

$$J = 1 + \frac{1}{N_t}\sum_{i=1}^{N_t}\sum_{j\neq i}\mathrm{E}\left\{\cos\left(\tilde{\phi}_i - \tilde{\phi}_j\right)\right\}$$

Under our assumptions, $\tilde{\phi}_i$ are identically distributed (but not independent) zero-mean Gaussian random variables with variance is $\sigma_\phi^2(t_p)$ and covariance $\mathrm{E}\left\{\tilde{\phi}_i\tilde{\phi}_j\right\} = \rho^2\sigma_\phi^2(t_p)$ at prediction time t_p. It can then be shown via straightforward integration that $\mathrm{E}\left\{\cos\left(\tilde{\phi}_i - \tilde{\phi}_j\right)\right\} = e^{-(1-\rho^2)\sigma_\phi^2(t_p)}$, hence

$$J = N_te^{-(1-\rho^2)\sigma_\phi^2(t_p)} + \left(1 - e^{-(1-\rho^2)\sigma_\phi^2(t_p)}\right). \quad (11)$$

Note that (11) is the mean beamforming power for a system with a single intended receiver and no nulls. If the system also steers nulls toward $N_r - 1$ receivers and the channel phases are random and independent, we can estimate the beamforming loss due to nulling as $1 - \frac{N_r-1}{N_t}$ [8]. Hence, it follows that

$$J \approx \left[1 - \frac{N_r - 1}{N_t}\right]N_te^{-(1-\rho^2)\sigma_\phi^2(t_p)} + 1 - e^{-(1-\rho^2)\sigma_\phi^2(t_p)}. \quad (12)$$

To quantify the performance of distributed *nullforming* at the protected receivers in terms of the prediction covariance, the signal from the i^{th} transmitter at a protected receiver is assumed to be given by $r_i = \alpha e^{j(\phi_i+\tilde{\phi}_i)}$ where ϕ_i is the nominal received phase from the

i^{th} transmitter chosen so that $\sum_{i=1}^{N_t} e^{j\phi_i} = 0$, and $\tilde{\phi}_i$ is the phase error at transmitter i. The mean received power in a null is then

$$K = \mathrm{E}\left\{\left|\sum_{i=1}^{N_t} r_i\right|^2\right\} = \frac{1}{N_t}\sum_{i=1}^{N_t}\mathrm{E}\left\{p_i^2+q_i^2\right\} + \frac{1}{N_t}\sum_{i=1}^{N_t}\sum_{j\neq i}\mathrm{E}\left\{p_i p_j + q_i q_j\right\}$$

where $p_i = \cos(\phi_i)\cos(\tilde{\phi}_i) - \sin(\phi_i)\sin(\tilde{\phi}_i)$ and $q_i = \cos(\phi_i)\sin(\tilde{\phi}_i) + \sin(\phi_i)\cos(\tilde{\phi}_i)$. Since $p_i^2 + q_i^2 = 1$ and $p_i p_j + q_i q_j = \cos(\phi_i - \phi_j)\cos(\tilde{\phi}_i - \tilde{\phi}_j) + \sin(\phi_i - \phi_j)\sin(\tilde{\phi}_i - \tilde{\phi}_j)$, we can write

$$K = 1 + \frac{1}{N_t}\sum_{i=1}^{N_t}\sum_{j\neq i}\cos(\phi_i - \phi_j)\mathrm{E}\left\{\cos(\tilde{\phi}_i - \tilde{\phi}_j)\right\} + \frac{1}{N_t}\sum_{i=1}^{N_t}\sum_{j\neq i}\sin(\phi_i - \phi_j)\mathrm{E}\left\{\sin(\tilde{\phi}_i - \tilde{\phi}_j)\right\}.$$

Straightforward integration yields $\mathrm{E}\left\{\cos(\tilde{\phi}_i - \tilde{\phi}_j)\right\} = e^{-(1-\rho^2)\sigma_\phi^2(t_p)}$ and $\mathrm{E}\left\{\sin(\tilde{\phi}_i - \tilde{\phi}_j)\right\} = 0$, hence

$$K = 1 + \frac{1}{N_t}e^{-(1-\rho^2)\sigma_\phi^2(t_p)}\sum_{i=1}^{N_t}\sum_{j\neq i}\cos(\phi_i - \phi_j)$$

It can be shown that, since ϕ_i satisfy $\sum_{i=1}^{N_t} e^{j\phi_i} = 0$, the sum $\sum_{i=1}^{N_t}\sum_{j\neq i}\cos(\phi_i - \phi_j) = -N_t$. Hence, the mean received power in a null is

$$K = 1 - e^{-(1-\rho^2)\sigma_\phi^2(t_p)}. \tag{13}$$

5. NUMERICAL RESULTS

This section presents numerical performance comparisons of distributed beamforming and nullforming with local and unified tracking. All of the results assume a forward link carrier frequency of 900 MHz and a measurement period of $T_m = 500$ ms. Based on the Allan variance specifications of the Rakon RFPO45 oscillator [14], the process noise parameters were set to $p_t^{(n)} = p_r^{(m)} = 2.31 \cdot 10^{-21}$ and $q_t^{(n)} = q_r^{(m)} = 6.80 \cdot 10^{-23}$ for all $n = 1, \ldots, N_t$ and all $m = 1, \ldots, N_r$. The standard deviation of the phase measurement error at the receive nodes was set to 10 degrees. All channels were assumed to have unit magnitude and the transmitter was assumed to have a unit total transmit power constraint.

Fig. 3 shows a full simulation of a "small" system with $N_t = 10$ transmitters and $N_r = 5$ receivers. Since the nullforming performance is identical at all of the protected receivers, the performance of only one null is shown here. The results were averaged over 3000 realizations of the random initial frequency offsets, clock process noises, and measurement noises. Measurements occur at $t = kT_m$ for $k = 0, 1, \ldots$. After the initial incoherent period where the Kalman filter has poor estimates with both local and unified tracking, the effect of the oscillator dynamics and periodic measurements can be seen in the beamforming and nullforming performance where the performance is relatively good immediately after a measurement but then degrades as the prediction time becomes longer. These results show that unified tracking provides a negligible advantage in beamforming gain but a potentially significant advantage in nullforming gain, especially as the Kalman filter converges to steady-state.

Figure 4 shows the steady-state performance of distributed beamforming and nullforming with local and unified tracking for the small system in Fig. 3 and a "massive MIMO" system with $N_t = 100$ transmitters and $N_r = 50$ receivers. These results were

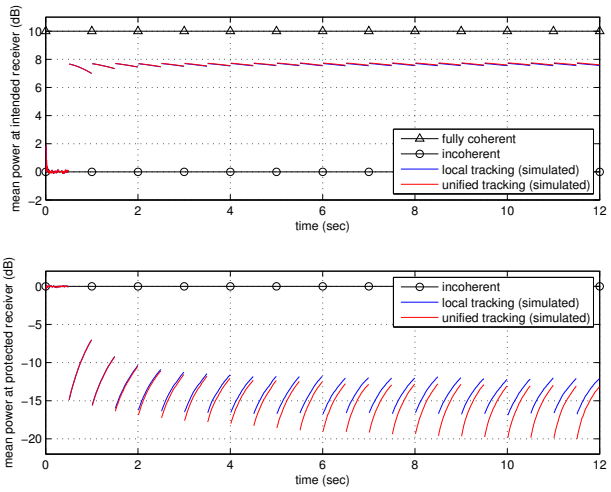

Fig. 3. Full Kalman filter simulation of a "small" system.

generated following the approach in Section 4. The small system results are consistent with Fig. 3. The massive MIMO system exhibits increased beamforming gain, as is expected, but also shows that beamforming performance is essentially the same with local or unified tracking. The nullforming performance of the massive MIMO system benefits more from unified tracking, especially over short prediction intervals. The nullforming performance of both systems becomes similar over longer prediction intervals.

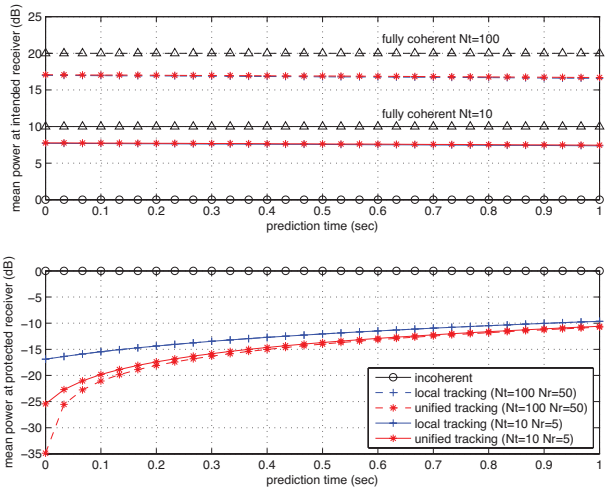

Fig. 4. Steady-state beamforming and nullforming performance results with "small" and "massive MIMO" systems.

6. CONCLUSIONS

This paper compares the performance of distributed transmission with local and unified tracking and shows that, while beamforming performance is effectively unchanged between local and unified tracking, nullforming performance can be significantly improved with unified tracking, especially over short prediction intervals and with larger networks. The results also show that local tracking tends to provide near-optimal performance in systems with high feedback latency. While unified tracking provides optimal performance, the additional complexity of unified tracking may cause local tracking to be more appealing in systems with high feedback latency.

7. REFERENCES

[1] R. Mudumbai, G. Barriac, and U. Madhow, "On the feasibility of distributed beamforming in wireless networks," *IEEE Trans. on Wireless Communications*, vol. 6, no. 5, pp. 1754–1763, May 2007.

[2] R. Mudumbai, D.R. Brown III, U. Madhow, and H.V. Poor, "Distributed transmit beamforming: Challenges and recent progress," *IEEE Comm. Mag.*, vol. 47, no. 2, pp. 102–110, Feb. 2009.

[3] R. Preuss and D. Brown, "Retrodirective distributed transmit beamforming with two-way source synchronization," in *Information Sciences and Systems (CISS), 2010 44th Annual Conference on*, march 2010, pp. 1 –6.

[4] R. Preuss and D.R. Brown III, "Two-way synchronization for coordinated multi-cell retrodirective downlink beamforming," *IEEE Trans. Signal Proc.*, vol. 59, no. 11, pp. 5415–27, Nov. 2011.

[5] D. Brown, P. Bidigare, and U. Madhow, "Receiver-coordinated distributed transmit beamforming with kinematic tracking," in *Acoustics, Speech and Signal Processing (ICASSP), 2012 IEEE International Conference on*, Mar. 2012, pp. 5209–5212.

[6] K. Zarifi, S. Affes, and A. Ghrayeb, "Collaborative null-steering beamforming for uniformly distributed wireless sensor networks," *IEEE Trans. on Signal Processing*, vol. 58, no. 3, pp. 1889 –1903, Mar. 2010.

[7] D.R. Brown III and U. Madhow, "Receiver-coordinated distributed transmit nullforming with channel state uncertainty," in *Conf. Inf. Sciences and Systems (CISS2012)*, Mar. 2012, to appear.

[8] D.R. Brown III, P. Bidigare, S. Dasgupta, and U. Madhow, "Receiver-coordinated zero-forcing distributed transmit null-forming," in *Statistical Signal Processing Workshop (SSP), 2012 IEEE*, Aug. 2012, pp. 269–272.

[9] J. Hoydis, S. ten Brink, and M. Debbah, "Massive mimo: How many antennas do we need?" in *Communication, Control, and Computing (Allerton), 2011 49th Annual Allerton Conference on*, 2011, pp. 545–550.

[10] E. G. Larsson, F. Tufvesson, O. Edfors, and T. L. Marzetta, "Massive mimo for next generation wireless systems," *submitted to IEEE Communications Magazine*, vol. abs/1304.6690, 2013.

[11] L. Galleani, "A tutorial on the 2-state model of the atomic clock noise," *Metrologia*, vol. 45, no. 6, pp. S175–S182, Dec. 2008.

[12] G. Giorgi and C. Narduzzi, "Performance analysis of kalman filter-based clock synchronization in IEEE 1588 networks," in *International IEEE Symposium on Precision Clock Synchronization for Measurement, Control, and Communication*, October 12-16 2009, pp. 1–6.

[13] Y. Bar-Shalom, X. R. Li, and T. Kirubarajan, *Estimation with Applications to Tracking and Navigation*. John Wiley and Sons, 2001.

[14] "Rakon RFPO45 SMD oven controlled crystal oscillator datasheet," 2009. [Online]. Available: http://www.rakon.com/Products/Public/Documents/ Specifications/RFPO45.pdf